ARTICLE NO. 80-4066

Theory, Simulation, and Practical Tests of a Counterspun Nutation Damper for Prolate Spinners

R. Annett,* W.J. Shackcloth,† and S.W. Tonkin‡
British Aerospace Dynamics Group, Bristol, U.K.

A nutation damper described in some previous papers is considered. It consists of a flywheel attached by a dissipative tilting mounting on the axle of a motor parallel to the spacecraft spin axis, but spinning in the opposite direction to the spacecraft. It is treated first by theory using differential equations applied to a quasi-steady-state showing that it stabilizes oblate and prolate spinners and that it fits into a comparatively unexplored corner of the field that is generally understood. As a result of the theory, some optimization is done and design goals suggested. The equations are simulated on an analog computer and some examination made of performance on spacecraft that are inertially more difficult to treat by theoretical means. Stabilization is demonstrated on triaxial prolate spacecraft and spherical spacecraft are made to spin about a preferred axis. A little success has been achieved with spacecraft spinning about an intermediate inertia axis. A rudimentary damper has been made and fitted to a prolate body with an inertia ratio of 0.6, mounted on a spherical air bearing. Stabilization is demonstrated and it is shown how the results relate to theory. There is some discussion of the shortcomings of the damper tested and probable methods of engineering for space.

Nomenclature

A = spacecraft transverse inertia
A' = flywheel transverse inertia
C = spacecraft spin inertia
C' = flywheel spin inertia
$\boldsymbol{h}$ = spacecraft angular momentum = $(A\omega_1, A\omega_2, Cr)^T$
$\boldsymbol{h}'$ = flywheel angular momentum = $(A'\omega_1', A'\omega_2', C(r+r'))^T$
$\boldsymbol{m}$ = viscous torque acting on the spacecraft
$\boldsymbol{m}'$ = viscous torque acting on the flywheel
r = spacecraft spin rate
r' = flywheel spin rate relative to spacecraft
x,y,z = spinning spacecraft axes
x',y',z' = flywheel axes
β = angle between angular momentum axis and flywheel axis
γ = phase lag of flywheel motion on spacecraft motion
Γ = transformation between spacecraft and flywheel axis sets
δ = angle between flywheel axis and motor axle
θ = spacecraft nutation angle
κ = coefficient of spring torque
λ = spacecraft inertia ratio = C/A
λ' = flywheel inertia ratio = C'/A'
μ = coefficient of viscous torque
ν = spacecraft nutation frequency in axes spinning with flywheel
ξ = flywheel transverse angular velocity
ρ = ratio of flywheel to spacecraft transverse angular velocities
τ = spacecraft nutation decay time constant
τ' = flywheel following time constant
ψ,ϕ,χ = Euler angles defining transform between spacecraft and flywheel
ω = angular velocity of spacecraft axes spinning with flywheel = $(\omega_1, \omega_2, r+r')^T$
ω' = flywheel angular velocity = $(\omega_1', \omega_2', r+r')^T$
$\dot{(\ )}$ = differentiation with respect to time
$(\ )^T$ = transpose
$\hat{(\ )}$ = unit vector

Presented as Papers 78-1312 and 78-1313 at the AIAA Guidance and Control Conference, Palo Alto, Calif., Aug. 7-9, 1978; submitted Sept. 15, 1978; revision received May 31, 1979.

Index category: Spacecraft Dynamics and Control.

*Systems Engineer, Space Systems.
†Head of Structural Dynamic Testing, Space Systems.
‡F.R.Ae.S., Assistant Chief Systems Engineer, Space Systems.

Introduction

IT is well known that energy dissipating components, such as tanks of propellant or flexing structure, cause instability in spinning rod-shaped (prolate) spacecraft while stabilizing flywheel-shaped (oblate) spacecraft. This principle can be more generally stated by saying that dissipative components on rotating platforms with positive nutation frequency are stabilizing, whereas they are destabilizing if the nutation frequency is negative. When the stabilization of prolate spinners began to exercise people's minds, this principle was used. Apparently there were some very early demonstrations by Kuebler, but one of the earliest documents on the subject was Ref. 1. Many references on the subject appeared and notable among these were Refs. 2 and 3. From these was developed the principle of stabilizing a prolate spinner by means of a dissipative device on a despun platform. This principle was used in Intelsat IV, Intelsat IVa, and using a slightly different principle, on Tacsat.[4]

Where no despun platform exists for other purposes, an active control system has been used. While such a system failed on ATS 5, it has been successfully used on many projects. Systems using gas jets as actuators are certainly more common,[5,6] but they suffer from the disadvantage that their efflux may do some damage impinging on another body and that they may tilt the angular momentum vector. An active system using a reaction wheel as the actuator[7] has been used, though it is a little heavy.

A corollary from the principle of giving a dissipator a positive nutation frequency was to counterspin a dissipator. A device was patented in early 1970.[8] Quite independently, it transpired that Cloutier of Hughes Aircraft was considering a device of the same type but differing in detail, and Kuebler patented a similar device,[9] although he did not state that it was to be counterspun. Cloutier read a paper[10] on a device differing radically in principle from the device discussed here, after Tonkin had submitted a paper.[11] References 12-15 came subsequently, and the present paper is a combination of Refs. 14 and 15.

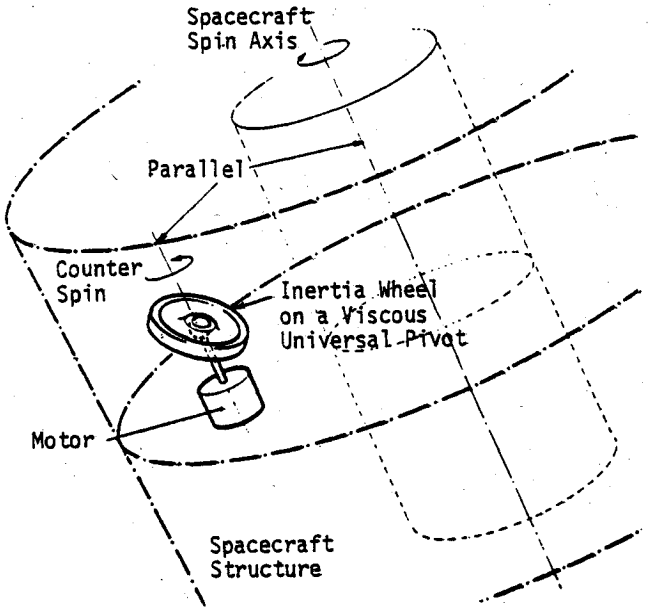

Fig. 1 Counterspun complaint flywheel.

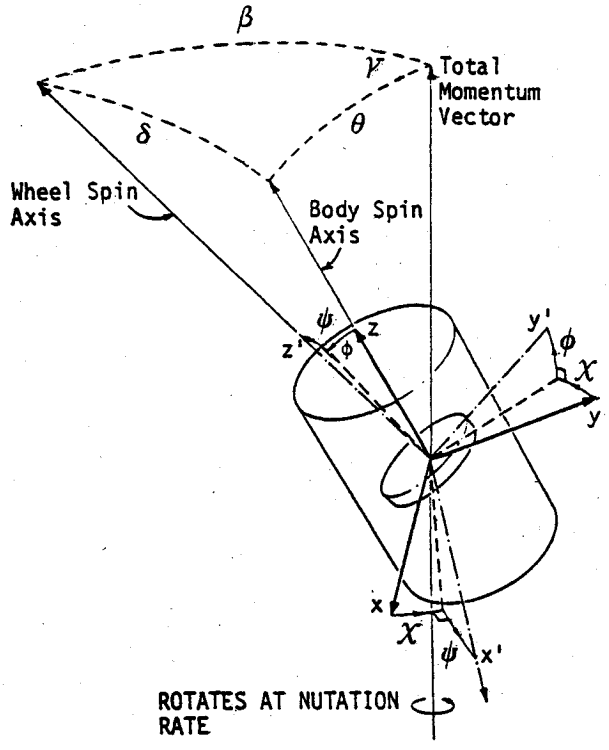

Fig. 2 Axes sets representation.

Although theory has been treated before using a vectorial, energy-sink, quasi-steady-state method, the present paper uses differential equations instead of the vectors and the energy sink. The equations developed were also put on an analog computer and some results are given. A very simple damper was built and fitted to a prolate spinner mounted on a three-axis air bearing. The results obtained were then compared with theory.

The basic layout of the device is shown in Fig. 1. The diagram shows the flywheel supported on a ball-joint, but consideration has also been given in the theory to the use of a Hooke's joint suspension with a chosen stiffness spring restraint tending to return the wheel to its undeflected position.

Analysis

The main body is assumed, for the sake of simplicity, to be a right circular cylinder with equal transverse inertias. This is not necessary to form soluble equations but does reduce the complexity of later algebraic manipulations. The motor axle is mounted parallel to the main-body principal axis of spin (misalignment causes a slight increase in motor power).

The ball of the ball-joint is assumed to be concentric with its housing with a small clearance between, which is flooded with a viscous fluid. This fluid causes torque to be transmitted by the ball-joint on the same axis as the slip angular velocity vector, which is $-\mu$ times this slip angular velocity. At the same time a spring restraint may be incorporated producing a torque on the same axis as the angular tilt of the wheel relative to its shaft, which is $-\kappa$ times this angular tilt. Engineering this spring may involve a Hooke's joint instead of a ball-joint. There may also be an extraneous Coulomb friction torque between the two parts of the ball-joint. Where this is considered it is assumed to be a torque of fixed amplitude on an axis parallel to the slip angular velocity, and of a sign which opposes such slip.

It is assumed that the wheel and motor speeds are equal. A little consideration will show that with only viscous torques the speed lag will be very small and stroboscopic examination shows that Coulomb friction makes the wheel turn with the motor.

Dynamic Equations

The dynamic equations are derived using the familiar Newton-Euler equation, but in an axis set with one axis coincident with that of the main body principal spin axes, but rotating at the same rate as the motor axle. The contribution to the overall spacecraft inertia from the flywheel is considered negligible. The flywheel is further taken to be spinning at constant rate r' with respect to the spacecraft main body.

The flywheel and spacecraft spinning axes are related through the small angle rotations χ,ϕ,ψ about the carried 3,1,2 axes, respectively, as shown in Fig. 2.

However, for the purpose of analysis, only a steady-state solution is required and hence χ is assumed 0. The tilt δ of the flywheel on the motor axle is the root square sum of ϕ and ψ. The small angle transformation (neglecting translation) is given by

$$\Gamma = \begin{bmatrix} 1 & 0 & -\psi \\ 0 & 1 & \phi \\ \psi & -\phi & 1 \end{bmatrix}$$

The angular momentum of the spacecraft in the spinning axes is given by

$$h = (A\omega_1, A\omega_2, Cr)^T \tag{1}$$

Similarly, the flywheel angular momentum is

$$h' \neq [A'\omega_1', A'\omega_2', C'(r+r')]^T \tag{2}$$

If m' and m are the viscous torques acting on the flywheel and spacecraft, respectively, then

$$m' = \mu(\Gamma\omega - \omega') \tag{3}$$

$$m = \mu(\Gamma^{-1}\omega' - \omega) \tag{4}$$

Similarly, the spring torques are equal and opposite and of the form

$$\text{Spring Torque} = \pm\kappa(\phi, \psi, 0)^T \tag{5}$$

Substituting Eqs. (1-5) in the Newton-Euler equations yields the following explicit relations:

$$A\dot{\omega}_1 + A\nu\omega_2 = \mu[\omega_1' - \omega_1 + \psi(r+r')] + \kappa\phi$$

$$A\dot{\omega}_2 - A\nu\omega_1 = \mu[\omega_2' - \omega_2 - \phi(r+r')] + \kappa\psi \qquad (6)$$

$$A'\dot{\omega}_1' + A'(\lambda'-1)(r+r')\omega_2' = \mu[\omega_1 - \omega_1' - \psi(r+r')] - \kappa\phi$$

$$A'\dot{\omega}_2' - A'(\lambda'-1)(r+r')\omega_1' = \mu[\omega_2 - \omega_2' - \phi(r+r')] - \kappa\psi \qquad (7)$$

ν is the body nutation frequency *as "seen" in the spinning axis set.*, i.e.,

$$\nu = r(\lambda - 1) - r' \qquad (8)$$

Note that this nutation frequency would have a slightly different value if the flywheel were rigidly attached to the shaft and the angular momentum of the wheel were comparable with that of the spacecraft.

For a first-order analysis it is usual to assume that the spacecraft spin rate remains constant, thereby allowing the spin axis equation to remain uncoupled from the transverse axes and, further, linearizing the transverse equations.

To complete the set of dynamic equations, a relation is required to define ϕ, ψ in terms of the angular rates. For small angles:

$$\dot{\psi} = \hat{z}' \cdot \hat{x} + \hat{z}' \cdot \hat{x} \qquad (9)$$

Substituting into Eq. (9) the correct values for the direction cosines of $\hat{x}$, $\hat{z}$, etc., the following relations are obtained:

$$\dot{\psi} = \omega_2' - \omega_2 - \phi(r+r')$$

$$\dot{\phi} = \omega_1' - \omega_1 + \psi(r+r') \qquad (10)$$

Pseudo-Steady-State Solution

To obtain analytic results a technique used by Flatley[16] was employed—the so-called pseudo-steady-state solution. The dominant motion is assumed to be due to the nutating main spacecraft. The spacecraft equations are solved in the torque-free case, the steady-state solution. This solution is inserted into the damper equations, retaining only the first-order and constant terms. It is assumed that the dominant change in the nutation angle of the spacecraft is due mainly to the constant terms. Oscillatory terms, typically those at wheel spin frequency and wheel nutation frequency, generate only small perturbations of the nutation angle about some mean value. The impact of the nutational motion on the damper is calculated, the result being reinserted into the body equations to generate the first-order motion of the body.

Solution of Eq. (6) in the absence of torque (i.e., terms on the right-hand side) yields

$$\omega_1 = \xi\cos\nu t \qquad \omega_2 = \xi\sin\nu t \qquad (11)$$

where ξ is the transverse velocity and ν, Eq. (8), is the body nutation frequency in axes spinning with the wheel.

A form of the solution for the flywheel angular rates is assumed, namely

$$\omega_1' = \rho\cos\gamma\omega_1 - \rho\sin\gamma\omega_2$$

$$\omega_2' = \rho\sin\gamma\omega_1 + \rho\cos\gamma\omega_2 \qquad (12)$$

Solving Eq. (10) in the absence of oscillatory terms using Eqs. (11) and (12) yields

$$\psi = (1/\lambda r)[\omega_1(-\rho\cos\gamma + 1) + \omega_2\rho\sin\gamma]$$

$$\phi = (1/\lambda r)[\omega_2(\rho\cos\gamma - 1) + \omega_1\rho\sin\gamma] \qquad (13)$$

Equation (13) can now be substituted into Eq. (7), including the torque terms, to establish the impact of the body motion on the wheel. Hence

$$\rho\sin\gamma\{(r+r')(C'-A') - \nu A' + \kappa/\lambda r\} = \mu[1 - (r+r')/\lambda r](1 - \rho\cos\gamma)$$

$$(\rho\cos\gamma - 1)\{(r+r')(C'-A') - \nu A' + \kappa/\lambda r\} = \mu[1 - (r+r')/\lambda r]\rho\sin\gamma - [(r+r')(C'-A') - \nu A'] \qquad (14)$$

Equations (14) can be usefully rearranged to give

$$\rho\cos\gamma - 1 = \frac{-[(r+r')(C'-A') - \nu A'][(r+r')(C'-A') - \nu A' + \kappa/\lambda r]}{[(r+r')(C'-A') - \nu A' + \kappa/\lambda r]^2 + \mu^2[1 - (r+r')/\lambda r]^2}$$

$$\rho\sin\gamma = \frac{\mu[1 - (r+r')/\lambda r][(r+r')(C'-A') - \nu A']}{[(r+r')(C'-A') - \nu A' + \kappa/\lambda r]^2 + \mu^2[1 - (r+r')/\lambda r]^2} \qquad (15)$$

If in Eq. (6) the torque terms are included, then

$$\tau = \omega_1/\dot{\omega}_1 = A\{\mu(\rho\cos\gamma - 1)[1 - (r+r')/\lambda r] + (\kappa/\lambda r)\rho\sin\gamma\}^{-1} \qquad (16)$$

The expressions for $\cos\gamma$ and $\sin\gamma$ as given in Eq. (15) are now substituted into Eq. (16), yielding an expression for the time constant τ, namely

$$\tau = \frac{-A\{[(r+r')(C'-A') - \nu A' + \kappa/\lambda r]^2 + \mu^2[1 - (r+r')/\lambda r]^2\}}{\mu[1 - (r+r')/\lambda r][(r+r')(C'-A') - \nu A']^2} \qquad (17)$$

Examination of the Solution

Equation (17) immediately yields the following points of interest: 1) the existence of an absolute stability domain; 2) an optimum choice of coefficient of viscosity μ, when there is no spring enhancement; 3) when there is spring enhancement and finite viscosity coefficient, the existence of an optimal coefficient of spring rate κ.

In Eq. (17) all but one of the terms are either defined positive or squared. Thus the condition for absolute stability is

$$r(\lambda - 1) - r' > 0 \qquad (18)$$

i.e., the nutation frequency in the axes of the dissipative body must be positive. This result agrees with the accepted stability criterion, for example the work of Bainum et al[17], on making the approximation that $A'/C \ll 1$, which was a previously stated approximation.

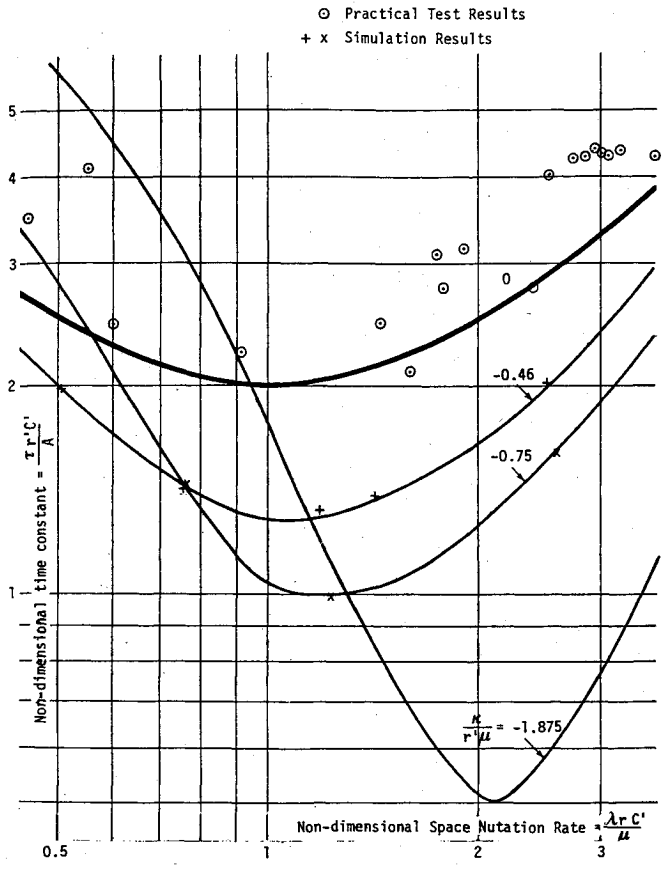

Fig. 3 Damper performance.

By setting the coefficient of spring rate to zero an expression for the optimum value of μ can be obtained, namely

$$\mu_{opt} = rA'\{1-(\lambda'-1)(r+r')/v\} \tag{19}$$

If $|r'/r| \gg 1$, then Eq. (19) reduces to

$$\mu_{opt} = \lambda r C' \quad \text{or} \quad I = \lambda r \times C'/\mu_{opt} \tag{20}$$

It will be seen later that the expression C'/μ is the following time constant of the wheel. Put into words, the product of the following time constant and the body nutation frequency in space should be unity.

Figure 3 is a plot of Eq. (17). The time constant τ is nondimensionalized by dividing by $A/r'C$. The nutation rate is nondimensionalized by multiplying by the following time constant C'/μ. The optimum of Eq. (20) can be seen in the case where $\kappa = 0$. Lines for three levels of spring enhancement are shown using the parameter $\kappa/r'\mu$ to define the amount of enhancement. It can also be seen that if κ and μ are manipulated the time constant can theoretically be made to approach zero. If an attempt is made to approach this desirable state of affairs, some of the approximations made in the theory break down. Besides this, as more and more spring enhancement is used, wheel tilt for a given nutation becomes difficult to accommodate and matching becomes sharper.

Behavior of the Damper on the Bench

A diagram of the damper with the motor fixed to the bench is shown in Fig. 4. The wheel is shown tilted an angle δ about some transverse axis. Due to the spring restraint, the wheel will be subject to a torque vector of magnitude $-\kappa\delta$. This torque will cause the wheel to precess at a rate $-\kappa\delta \times r'/C'r'^2$, which is in such a direction that it does not change δ. As the wheel and motor axle are spinning at the same rate r' the relative spin at the ball-joint will be $\delta \times r'$. This relative spin will be opposed by a torque $-\mu\delta \times r'$,

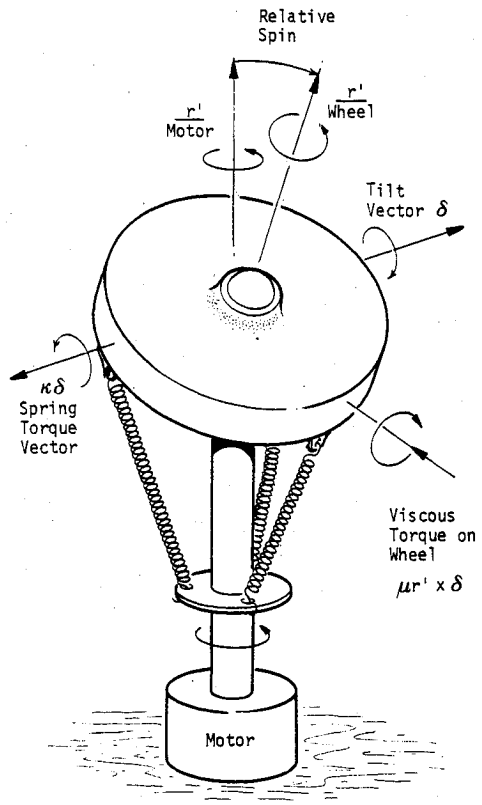

Fig. 4 Damper mounted on bench.

and this torque will precess the wheel at a rate of $\cdot(-\mu\delta \times r') \times r'/C'r'^2$. The axis of this precession vector happens to coincide with the tilt vector and it is negative and proportional to it. Thus the decay of tilt will be exponential with a time constant $\tau' = C'/\mu$ the "following time constant" mentioned previously.

If the friction torque were caused by Coulomb friction it would be on the same axis as the viscous torque but of a magnitude independent of the tilt. The resulting precession rate would be constant until slipping at the ball ceases.

Computer Simulation and Results

To verify the theoretical analysis an analog computer simulation of an extended set of dynamic equations was set up. The simulation included: 1) a Hooke's joint suspension unit, 2) nonzero spider inertias, 3) spring enhancement, 4) dc and hysteresis motors, with speed loss according to load, 5) fuel swirl, and 6) misalignment with the body principal axis. In several respects, the simulation covered a more complex case than that treated by theory.

The modeling of the Hooke's joint was thought to represent a more likely path for the development of the damper. The nonzero spider inertias were included to assess the impact of possible vibrations from the damper on the main-body, and to obtain the negative spring rate which they produce.

The dynamic equations were derived from momenta considerations. By calculating the momentum of individual components and summing all the momenta, a constraint exists that the total angular momentum must be constant. This enables the equations to be derived in a closed-loop form and hence prevent the drift inherent in analog simulations. The bandwidth of the system is large, including spin rates up to 500 rad/s together with nutation frequencies of 0.1 rad/s.

An open-loop set of equations proved to be so sensitive to startup transients as to negate its use for simulation purposes.

The output of the simulation was an xy plot of the two transverse spin rates plus a multichannel recording showing various parameters such as body nutation angle, wheel tilt, wheel lag, wheel speed (the speed drop on load depended on

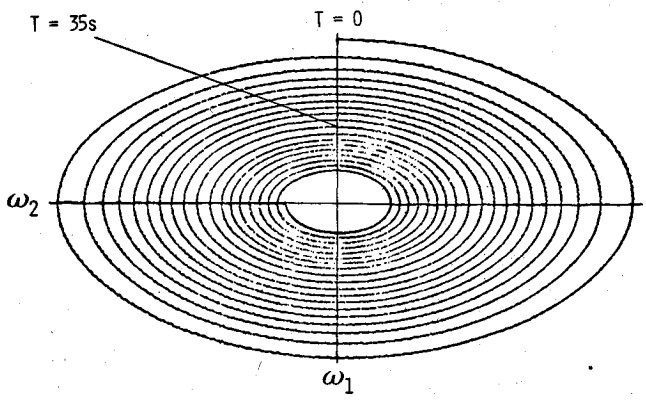

Fig. 5 Counterspinning damper on prolate body with unequal transverse inertias.

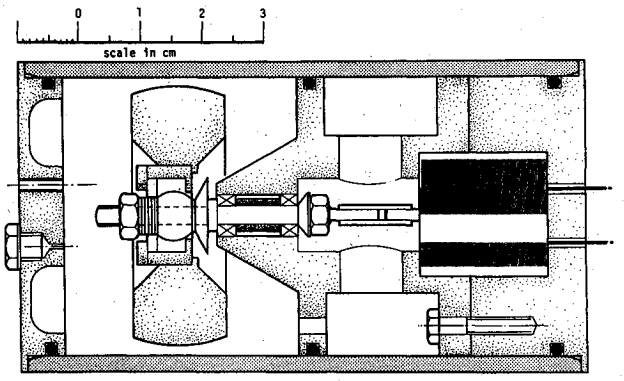

Fig. 6 The damper tested.

the type of motor), etc. The multichannel recordings do not lend themselves to reproduction, but a typical *xy* plot is reproduced in Fig. 5. It shows the transverse spin rates in body axes for a prolate spacecraft having differing moments of inertia about the two transverse axes.

A spherical body was tried, initially spinning about an oblique axis, and the damper caused it to reorientate itself to spin about an axis parallel to the motor axle. A trial spinning about the intermediate axis of a triaxial body was unsuccessful. However a variable geometry body was tried with differing transverse inertias, and it passed from prolate to oblate, through the unstable region, without mishap.

Some of the results of the simulation are superimposed onto the theoretical plots of Fig. 3. For two of the levels of spring enhancement the results are plotted as crosses.

Practical Testing

The Damper

A simple damper was made and is shown in Fig. 6. The motor was a 20 mm Faulhaber 1.5 V dc motor which drove the wheel at various speeds between 4000 and 10,000 rpm according to conditions, but commonly around 8000 rpm. The flywheel was of brass, with an outside diameter of 42 mm, a mass of 0.131 kg, and a moment of inertia of 3.39×10^{-5} kg-m^2 (originally estimated at 3.786×10^{-5}kg-m^2).

The mounting of the flywheel included viscosity but no spring constraint. The mounting was a Rose MBB 3 spherical bearing. Care was taken that the center of mass of the flywheel was at the center of the ball in the axial sense as well as the more obvious radial sense. The bearing was encased to prevent loss of lubricant and a felt pad included as a reservoir. The ball was burnished with molybdenum disulphide in an attempt to reduce Coulomb friction and lubricated with oil of viscosity 725 CP at 15° C. Bearing clearance was not known, so no calculations could be made on viscosity. Note that as the bearing was spherical the clearance affected eccentric running and the effects of the viscous lubricant, but played no part in holding the wheel normal to the motor axle.

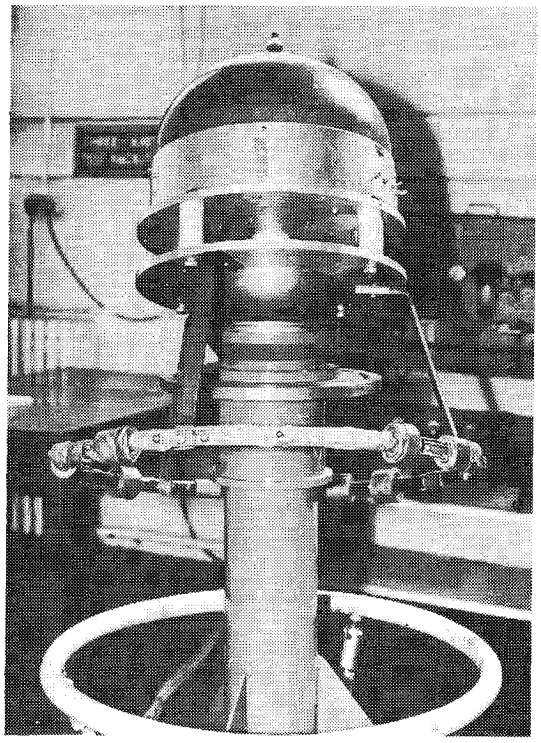

Fig. 7 General view of "satellite" body.

Provision was made to pump down the damper casing to reduce windage losses, but this was not found to be necessary. It is not suggested that the damper as engineered would have any application in space, as various aspects, particularly the method of generating viscous torques, would be quite unsatisfactory in space. It was originally made for a demonstration.

The "Satellite" Body

The "satellite" body is shown in Fig. 7. It was supported by a 5-in. radius spherical air bearing. The upper part, containing the damper, batteries and various other components, together with a large mass, was kept as compact as possible. It was encased in a spherical fairing to reduce aerodynamic forces as much as possible. The damper was mounted some distance from the center of mass and about 6 in. off the spin axis. No special precautions were taken to ensure that the motor axle was parallel to the spin axis. The lower loop was merely ballast to bring the center of mass down to coincide with the center of the air bearing. The main ballast was lead wound around the hoop, but the balance was trimmed by adding modeling clay and bearing balls.

Static balancing was achieved by removing the mass from the hoop to lengthen steadily the natural period of pendulous oscillation while keeping the oscillation symmetrical about the vertical. Dynamic balancing made use of the instrumentation and will be described later.

The transverse moment of inertia was measured by unifilar suspension. The inertia ratio was measured by measuring the ratio between spin period and nutation period. The moments of inertia were spin, 1.14 kg-m^2, and transverse, 1.9 kg-m^2. It can be seen that the "satellite" was well and truly prolate.

The "satellite" was either spun up directly by hand or with a cord to speeds of 1-2 rev/s. Nutation was simply initiated by a judicious blow with the hand. A vacuum chamber was not used, simply because a large enough one was not available. Aerodynamic torques were not small and had to be compensated for by a lengthy process. It was obvious beforehand

that a vacuum chamber was desirable and if further tests are done, one will be used.

Measurement Methods

Moment of Inertia

As already mentioned, a unifilar suspension was used.

Body Motion

The body was fitted with a battery-driven flashlight bulb mounted on the spin axis. It was viewed by a TV camera directly overhead and as it was useful in some cases, the TV signal was recorded so that it could be played back frame-by-frame. Nutation rate and amplitude could be obtained from the circular motion of the spin-axis flashlight bulb. However the bulb had to be mounted on the principal axis, in other words the body had to be dynamically balanced. The body had been kept as symmetrical as possible so that the discrepancy between geometric axis and principal axis was not large. However, when the bulb performed the combination of coning at spin speed and nutation, it did a hesitant cusping motion. By marking the motion on the TV screen and examining the locus in conjunction with the still it is possible to deduce where the principal axis is and move the bulb to the correct position. After finding the principal axis the motor axle should have been realigned, but the discrepancy was so small it was not considered necessary to bother.

Spin rate was obtained by observing rotation of the body and timing it with a stop-clock.

Damper Flywheel Tilt

It was necessary for test purposes to know the flywheel tilt on the motor axle, and to know the wheel speed. Both these were obtained from the signal from a photoelectric probe looking at a shark's-tooth pattern on the wheel rim. Frequency gave speed and mark/space ratio gave tilt. As no telemetry was used, tilt could not be measured on the "satellite." Speed was measured by amplifying the probe signal and feeding it to a loudspeaker. The note was compared with that from a loudspeaker on a calibrated oscillator.

To measure damper characteristics the damper was mounted to pivot about a horizontal axis coming against a stop so that the motor axle was then vertical. With the deflection recording system operating the damper was then rotated sharply to hit the stop and the deflection recorded.

Test Runs

Three types of tests were done: 1) damper not running, 2) damper counterspun, and 3) damper forward spun. For each run, the body would be spun up and nutation initiated. Measurements of 1) body spin speed, 2) body nutation angle, and 3) wheel spin speed, were taken at 1-min intervals until the nutation angle became very small or very large. In initiating runs an attempt was made to cover as wide a range of spin rates as possible. An attempt was also made to obtain results at a range of amplitudes at each spin rate. Whenever runs were done using the running damper the damper was taken off and its characteristics measured using the rig described earlier.

The effect which was not noticed was the rotation of the laboratory at Earth rate. This was probably because runs were fairly short and tests were done at U.K. latitude.

Discussion of Results

Figure 8 shows the results of three typical runs. Note that these results are not directly comparable because they covered different spin speed ranges. It is immediately apparent from the nutation decay with the wheel not running and from the decay of spin speed, which is not shown on Fig. 8, that some drag is occurring. Estimates were made of air bearing drag and runs were tried with double air pressure to the bearing. The conclusion was that this was the expected result of not working in a vacuum chamber, being due to aerodynamic drag forces.

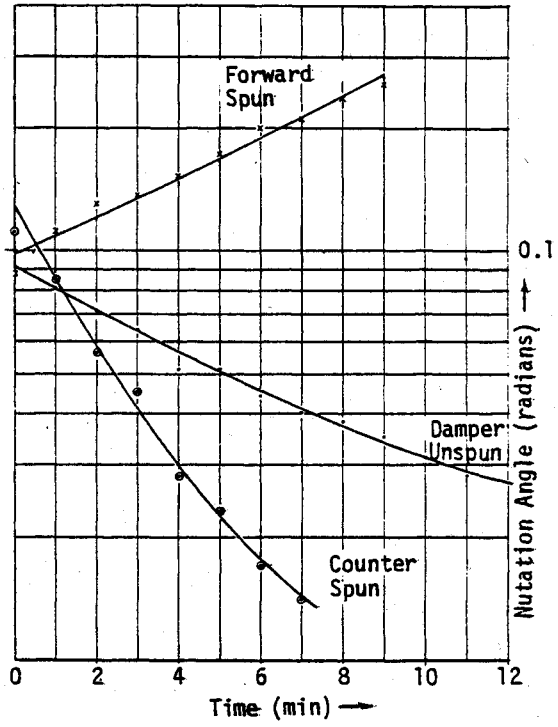

Fig. 8 Preliminary result of damper.

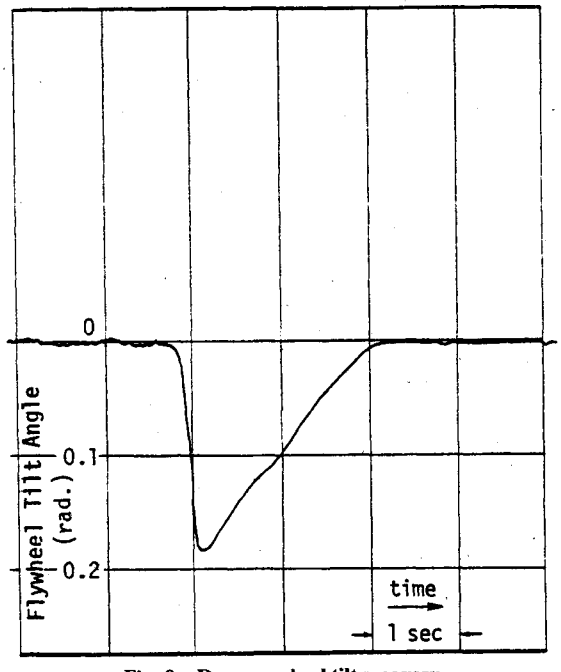

Fig. 9 Damper wheel tilt recovery.

Incidentaly, it may seem anomalous that damping (due to aerodynamics) causes a decay of nutation, when damping (perhaps due to fuel slosh) in space causes an expansion of nutation in a prolate body, which this is. This is completely in accordance with theory, the difference being that aerodynamics is Earth-based and does not operate with a conservation of angular momentum.

Figure 8 shows the effect of the damper. In one plot the damper is not running, and the nutation decay is due to aerodynamics. In another plot the damper is counterspun and the nutation decays more quickly. In the third plot the damper is forward spun and the resulting instability, predicted by

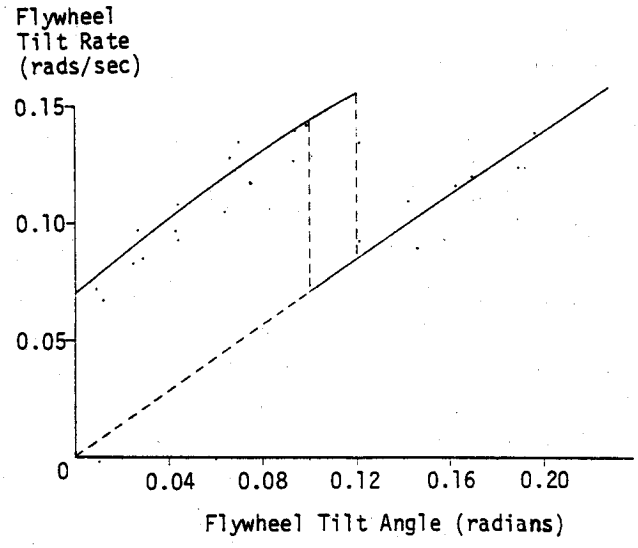

Fig. 10 Damper characteristics.

theory is powerful enough to overcome the aerodynamic damping.

Damping Behavior on Its Own

A typical trace obtained on the damper rig is shown in Fig. 9. From it and others like it, Fig. 10 is obtained. For a good understanding of their meaning it is well to be familiar with the section "Behavior of the Damper on the Bench."

For a perfectly engineered damper, producing only viscous drag torques, Fig. 9 should be a decaying exponential. It can be seen that this is very far from the case. From it, Fig. 10 was plotted, showing flywheel tilt rate against tilt angle. The result, while being unexpected, is highly informative.

If drag torque were only viscous, giving a decaying exponential for Fig. 9, Fig. 10 would be a straight line passing through the origin. The inverse of the slope of this line would then give the parameter "following time constant," which has to equal the inverse of body nutation rate for correct matching. In a nonlinear system the equivalent to following time constant is the quotient of the abscissa and the ordinate for any point at which the damper is operating. Except in the case where the characteristic of Fig. 10 is a straight line passing through the origin, this quotient will vary with amplitude, so that matching will vary with amplitude.

An obvious cause of departure from the desirable straight line through the origin on Fig. 10 is Coulomb friction. Coulomb friction on its own will give a horizontal line at a fixed finite level. The combination of Coulomb friction and viscous friction will give a line of constant slope but starting at a finite level. In either case, Coulomb friction causes matching to vary with amplitude.

It has previously shown[13] that Coulomb friction causes threshold, which in itself is undesirable. However this shift in matching with amplitude is even less desirable. These facts were probably not realized when Ref. 9 was written, because it advocates, as the sole means of energy dissipation, friction linings clamped on either side of the ball.

In the present case the lower part of Fig. 10 looks like the combination of Coulomb and viscous friction. At about 0.1 rad tilt there is a discontinuity and the characteristic from then on seems to show pure viscosity. It seems likely that above 0.1 rad tilt, natural lubricant pumping lifts the weight of the wheel and prevents metal-to-metal contact.

It can also be seen that low nutation rates and low nutation amplitudes, producing tilt rates of less than 0.07 rad/s, will not cause the flywheel to tilt and will therefore be undamped. This will represent the threshold of the device.

Damper Performance

Having seen that the damper works (Fig. 8) its performance must be checked quantitatively. It is proposed to indicate performace by plotting points indicating regime of operation on Fig. 3 so that they can be directly compared with theory.

The parameter plotted on the vertical scale is time constant nondimensionalized by dividing by $A/r'C'$. A, the satellite transverse inertia, and C', wheel moment of inertia are known. The flywheel spin rate r' is quite accurately obtained from the loudspeaker. However, the time constant due to the damper is a little more difficult to extract from the measured results.

Runs were done without the damper running for a variety of spin speeds and amplitudes, so that it was possible under any conditions to interpolate and deduce the natural contraction time constant due to aerodynamics. For a run with the damper spinning it was then possible to deduce the effect due to the damper alone.

For the horizontal scale of Fig. 3, which is the product of the nutation rate and the following time constant, the nutation rate is obtained very simply from the spin rate and the known inertia ratio of the satellite. Since the performance of the damper has been shown to be nonlinear we must replace following time constant with the quotient of abscissa and ordinate of Fig. 10 for the operating condition. As there was no telemetry giving wheel tilt angle the angle has to be estimated from the known nutation angle at any instant.

It is thus possible to reduce data obtained during test runs to points on Fig. 3. These are plotted as encircled points and can be compared at once with the theoretical result. It must be agreed at once that there is a great deal of random scatter. This is almost certainly due to the large number of processes in the reduction, because of the aerodynamic effects and Coulomb friction causing damper nonlinearity. The reason for high time constants at low nutation rates is because of the onset of damper threshold due to Coulomb friction. The most encouraging feature is that the order of theoretical depth of trough is attained. This shows unequivocally that a properly matched damper of given angular momentum can achieve the theoretical time constant on a spacecraft of given size.

Notes on Construction for Space Use

The most serious snags about the type of construction used are in the universal joint, the method of generating the viscous forces and the total lack of spring restraint. A Hooke's joint would be used instead of a ball-joint. Crossed spring pivots could be used in the Hooke's joint, but these have not proved very reliable under vibration. Ball-bearing pivots would probably have low enough Coulomb friction, and then torsion bars on pivot axes used to give spring restraint and eliminate bearing shake.

Viscous fluids do not give predictable values of viscous coefficients. Eddy currents have been investigated as an alternative method and it has been found that suitable components fit in nicely. A light alloy part spherical shell would be mounted rigidly on the motor axle, being enveloped by the flywheel rim. In the flywheel rim, a number of samarium cobalt permanent magnets can be mounted, which will generate eddy currents in the shell and produce the necessary viscous torques.

Apart from the universal mounting and the eddy current damping, construction techniques can be very similar to those for momentum wheels. For a SSUS D with payload, three units of 5 Nms angular momentum each will give quite adequate performance with one unit failed. Each 5 Nms unit would use a wheel 20 cm in diameter running at 5000 rpm.

Conclusions

The counterspun flywheel nutation damper described in previous references has been re-examined by a different type of theory, by analog computer, and in practical tests. All have

given results of the same type as previous theory and have increased confidence in the prediction of the performance of a given size damper.

Consideration of practical applications have shown that a suitable set of units would be of quite reasonable size.

Acknowledgments

The theoretical study was originally done under contract to the European Space Agency and the practical experiments done as a private venture by British Aerospace Dynamics Group. The authors are grateful to these two bodies for permission to publish the work and to many colleagues who have given useful advice. Thanks for useful comments are particularly due to William J. Russell of Aerospace Corp. and Bruce Bromberg of NASA Goddard Space Flight Center.

References

[1] Landon, V.D., "The Rotational Stability of a Body Containing a Rotor," RCA internal rept., circa 1962.

[2] Landon, V.D. and Stewart, B., "Nutational Stability of an Axisymmetric Body Containing a Rotor," *Journal of Spacecraft and Rockets,* Vol. 1, Nov.-Dec. 1964, pp. 682-684.

[3] Iorillo, A.J., "Nutation Damped Stabilised Device," U.S. Patent 3,442,468, original application date—July 1966.

[4] Johnson, C.R. "TACSAT 1 Nutation Dynamics," AIAA Paper 70-455, 3rd Communication Satellite Conference, 1970.

[5] Conolly, A., "An Active Control System for a Spinning Spacecraft," *Proceedings of the Symposium on Attitude Stabilisation and Control of Dualspin Spacecraft,* Report No. SAMSO-TR-68-191, Nov. 1967, pp. 111-118.

[6] Grashoff, L.H., "An On-board Closed-loop Nutation Control System for a Spin-Stabilized Spacecraft," *Journal of Spacecraft and Rockets,* Vol. 5, May 1968, pp. 530-535.

[7] Abercrombie, R.A. and Flatley, T.W., "Active Nutation Damping for Spacecraft," NASA TP 1108, 1978.

[8] Tonkin, S.W., "Improvements Relating to Spacecraft Provided with Nutation Dampers," UK Patent No. 1,344,256, application date—March 1970.

[9] Kuebler, M., "Dampfungseinrichtung an Satelliten," Deutsches Patentampt Nr. 1952280, Oct. 1969.

[10] Cloutier, G.J., "Variable Spin Rate, Two Degrees of Freedom, Nutation Damper Dynamics," *Proceedings of Astrodynamcis Specialist Conference,* AAS and AIAA, July 1975.

[11] Tonkin, S.W., "A Semi-active Nutation Damper for Spinning Oblate or Prolate Satellites," *Proceedings of the VIIth Symposium on Automatic Control in Space,* International Federation of Automatic Control, May 1976, pp. 207-226.

[12] Tonkin, S.W., "Non-active Nutation Damping for Single-spin Spacecraft of All Mass Distributions," *Aeronautical Journal of the Royal Aeronautical Society,* Sept. 1976, pp. 394-401.

[13] Simpson, J. and Annett, R., "Investigation of the Application of BAC Counterspun Nutation Damper for ESA Satellites," ESA Contract Rept. 2941/76.

[14] Tonkin, S.W. and Shackcloth, W.J., "Practical Test Behaviour of a Counterspun Flywheel Nutation Damper on a Spinning Prolate Body," AIAA Paper 78-1312, Guidance and Control Conference, Aug. 1978.

[15] Annett, R., "Theoretical Investigation of a Counterspun Compliant Flywheel Nutation Damper for Oblate and Prolate Spinning Spacecraft," AIAA Paper No. 78-1313, Guidance and Control Conference, Aug. 1978.

[16] Flatley, T.W., "Equilibrium States for a Class of Dual-spin Spacecraft," NASA TR-R-362, March 1971.

[17] Bainum, P.M., Feuchsel, P.G., and Fedor, J.V., "Stability of a Dual-spin Spacecraft with a Flexible Momentum Wheel," *Journal of Spacecraft and Rockets,* Vol. 9, Sept. 1972, pp. 640-646.